Journal of *Marine Science and Engineering*

MDPI

Article

UUV Cluster Distributed Navigation Fusion Positioning Method with Information Geometry

Lingling Zhang [1], Shijiao Wu [1], Chengkai Tang [2,3,*] and Hechen Lin [4]

[1] The School of Marine Science and Technology, Northwestern Polytechnical University, Xi'an 710072, China; llzhang@nwpu.edu.cn (L.Z.); wushijiao@mail.nwpu.edu.cn (S.W.)
[2] The School of Electronics and Information, Northwestern Polytechnical University, Xi'an 710072, China
[3] Research & Development Institute of Northwestern Polytechnical University in Shenzhen, Shenzheng 518063, China
[4] Eastern Michigan Joint College of Engineering, Beibu Gulf University, Qinzhou 535011, China; 2219403157@stu.bbgu.edu.cn
* Correspondence: cktang@nwpu.edu.cn; Tel.: +86-18629264785

Abstract: The development and utilization of marine resources by humanity are increasing rapidly, and a single unmanned underwater vehicle (UUV) is insufficient to meet the demands of ocean exploitation. Large-scale UUV swarms present a primary solution; however, challenges such as underwater mountain ranges and signal attenuation critically impact the real-time collaborative positioning and autonomous clustering abilities of these swarms, posing major issues for their practical application. To address these challenges, this paper proposes a UUV cluster distributed navigation fusion positioning method with information geometry (UCDFP). This method transforms the navigation data of individual UUVs into an information geometric probability model, thereby reducing the impact of temporal asynchrony-induced positioning errors. By integrating factor graph theory and utilizing ranging information between UUVs, a distributed collaborative fusion positioning architecture for UUV swarms is established, enabling seamless dispersion and regrouping. In experimental evaluations, the proposed method is compared with existing techniques concerning convergence speed and the capability of UUV swarms for autonomous dispersion and regrouping. The results indicate that the method proposed in this paper achieves faster convergence and higher positioning stability during the autonomous clustering of UUV swarms, marking a notable advancement in underwater vehicular technology.

Keywords: unmanned vehicle clusters; factor graph; fusion positioning; information geometry; underwater

check for updates

Academic Editor: Rafael Morales

Received: 10 February 2025
Revised: 27 March 2025
Accepted: 27 March 2025
Published: 31 March 2025

Citation: Zhang, L.; Wu, S.; Tang, C.; Lin, H. UUV Cluster Distributed Navigation Fusion Positioning Method with Information Geometry. *J. Mar. Sci. Eng.* **2025**, *13*, 696. https://doi.org/10.3390/jmse13040696

Copyright: © 2025 by the authors. Licensee MDPI, Basel, Switzerland. This article is an open access article distributed under the terms and conditions of the Creative Commons Attribution (CC BY) license (https://creativecommons.org/licenses/by/4.0/).

1. Introduction

With the rapid development of human science and technology, the utilization capability of marine resources has significantly improved. Unmanned underwater vehicles (UUVs) have become core equipment in fields such as marine exploration, resource development, and environmental monitoring due to their convenience and safety [1–3]. However, a single underwater vehicle is no longer able to meet the practical requirements of marine resource development due to limitations in endurance range and detection device coverage [4]. Therefore, the main direction of development is to form clusters of UUVs. In UUV clusters, the relative cooperative positioning among UUVs is the fundamental basis for UUV cluster applications. However, factors such as underwater mountains obstructing signals, underwater

signal attenuation characteristics, multipath effects, and other factors result in low real-time positioning accuracy for UUV clusters. Additionally, existing cooperative positioning technologies require stable networks and cannot meet the requirements for the free aggregation and dispersion of UUV clusters [5]. Therefore, it is imperative to develop UUV cluster cooperative positioning with high real-time performance and free aggregation capability.

Early UUV positioning relied on methods such as inertial navigation [6], sonar positioning [7], and underwater base stations [8]. However, factors such as sensor errors, communication limitations, and geographical constraints in the underwater environment resulted in low positioning accuracy. UUV clusters can effectively improve positioning accuracy through cooperative ranging between UUVs, but they require relatively stable cooperative networks. However, UUV clusters are unable to maintain stable cooperative networks due to underwater mountains and limited signal transmission distances [9]. Additionally, due to the mobility of UUVs, the number and positions within the UUV cluster exhibit significant free aggregation and dispersion characteristics. To address this, many researchers have introduced factor graph techniques into UUV cluster cooperative positioning [10–12]. This technique can meet the requirements of free aggregation and dispersion in UUV cluster cooperative positioning. However, the asynchronous nature of UUVs leads to a sharp decrease in positioning accuracy.

In order to attain high-precision positioning for UUV swarms, many researchers have explored the use of Kalman filtering and neural network techniques derived from wireless positioning networks for the collaborative positioning of UUV clusters. However, the Kalman filter's reliance on stable positioning networks and neural networks' high computational costs and bandwidth demands render both methods unsuitable for real-time positioning in UUV swarms. In response to the above issues, this paper proposes an unmanned underwater vehicle cluster cooperative fusion positioning method based on information geometry. The main innovations are as follows:

1. An information geometry probabilistic model of underwater navigation for UUVs was established, achieving the standardization of navigation information parameters among UUVs and reducing the impact of asynchronous timing on positioning errors.
2. Addressing the issues of poor real-time positioning and the inability to freely aggregate and disperse UUVs, a UUV cooperative positioning method based on information geometry probabilistic fusion was developed, combining the factor graph approach. This method utilizes the information geometry probability of each UUV as positioning information and constructs an information geometry probability factor graph fusion architecture, enabling real-time and high-precision positioning of UUV clusters.
3. A testing platform for UUV cluster cooperative fusion positioning was established, and experiments were conducted to evaluate the proposed method under scenarios involving sudden changes in positioning errors and free aggregation and dispersion of UUV clusters. The experimental results matched the simulation results, demonstrating that the proposed unmanned underwater vehicle cluster cooperative fusion positioning method based on information geometry can meet the requirements of real-time positioning and free aggregation and dispersion characteristics of UUV clusters.

The structure of this paper is as follows. In Section 1, common methods for unmanned underwater vehicle (UUV) cluster positioning are introduced, and their advantages and disadvantages are analyzed. Section 2 presents the related work on the underwater positioning of UUV clusters. Section 3 provides the mathematical derivation and theoretical process of the information geometry probabilistic fusion model. By combining the range measurements between UUVs and their own positioning information, a distributed positioning model for information probability fusion among underwater cluster sources is constructed. The cooperation positioning is achieved using factor graphs and the product

rule. Section 4 describes the simulation and analysis of UUV cluster cooperative positioning. In Section 5, experimental verification of UUV cluster cooperative positioning is conducted.

2. Related Work

2.1. Current Research Status at Home and Abroad

Due to the complexity of the underwater environment, unmanned underwater vehicles (UUVs) have been the primary tools for underwater exploration. In the early stages of underwater development, due to limitations in range, visual search, and underwater communication technology, single-vehicle operations were predominant [13]. The core basic positioning technologies for UUVs primarily relied on inertial navigation and sonar positioning. Radio positioning technologies, represented by satellite navigation, face significant challenges in achieving underwater positioning due to factors such as low power and poor penetration capabilities [14]. Later, methods such as depth sensor positioning [15], landmark recognition, and matching positioning were introduced [16]. However, these single-point positioning methods suffer from issues such as cumulative errors, environmental limitations, and lack of robustness, resulting in limited positioning accuracy.

Among these methods, the least squares (LS) approach has been widely used for UUV positioning fusion. Based on the modeling of the navigation error of the UUV, Zhang and An [17] introduced a least squares estimation method to compensate for the navigation error, in which the azimuth of the UUV achieved by the sensors on the mother ship is used. However, the LS method estimates the position of the UUV by minimizing the sum of squared observation errors, leading to a significant decrease in positioning accuracy when any navigation source experiences an error.

With the widespread application of the Internet of Things (IoT) on UUVs, UUVs are gradually transitioning from single-vehicle operations to cluster-based development. Zhuo Xiaoxiao and colleagues from the College of Oceanography at Zhejiang University explored the optimization of energy efficiency in underwater acoustic sensor networks through the assistance of autonomous underwater vehicles (AUVs) within the context of underwater IoT, addressing issues related to positioning and data collection in underwater clusters [18]. Meanwhile, Professor Yuan Fei's team at Xiamen University proposed a dual-dimensional underwater LoRa modulation method tailored for underwater IoT applications. Although their work does not directly address the positioning of underwater clusters, it provides a technical foundation and conceptual insights for related research [19]. In UUV clusters, cooperative positioning becomes the fundamental core of underwater applications. By enabling multiple UUVs to work together, wider task coverage and higher work efficiency can be achieved. However, the application of UUV clusters presents new challenges [20]. In the early stages, UUV cooperative positioning was similar to single-vehicle positioning, mainly relying on LS fusion of positioning data between neighboring UUVs. Subsequently, Ranjan, Arun, and Gajanan [21] proposed an underwater robot positioning method based on extended Kalman filtering (EKF), which achieved positioning of UUV clusters. However, the aforementioned methods exhibit obvious centralization. When UUVs operate underwater, they are easily affected by underwater topography, ocean currents, and communication obstacles, making centralized positioning networks unsuitable for underwater UUV clusters. Therefore, the development of distributed UUV cluster navigation and positioning is urgently needed.

In the early stages of UUV distributed cooperative positioning, researchers mainly introduced Kalman filtering into UUV cluster positioning. Zhang, Wu, and Ma [22] explored the application of the EKF algorithm for positioning on underwater vehicles. Bai, Huang, and Chen [23] proposed a robust Kalman filter based on Mixture Distributions (MDRKF) for cooperative positioning of autonomous underwater vehicles (AUVs). Experimental

results in a lake environment showed that the MDRKF method achieved better positioning accuracy, but it had higher computational complexity compared to existing state-of-the-art filtering algorithms. Ullah, Shen, and Su [24] proposed a modified Kalman filter (KF) based on the Unscented Kalman Filter (UKF) and particle filter (PF) for positioning. The robustness of the proposed algorithm was validated through numerical simulations. However, Kalman filtering requires significant computational resources and higher communication rates. The low communication rates between UUV clusters severely limit the improvement of positioning performance.

With the rapid development of deep learning, many researchers have introduced neural network fusion architectures into UUV cluster cooperative positioning. Wang, Xiang, and Guan [25] proposed a deep neural network-based method for autonomous underwater robot positioning. The neural network was trained to estimate the robot's position, and the algorithm's performance was validated through experiments. Peng, Zhang, and Xu [26] proposed a deep learning-based method for underwater multi-robot positioning. They utilized deep neural networks to process sonar data and conducted experiments to study the accuracy and robustness of the algorithm. Zhu and Kia [27] introduced a measurement scheduling method for cooperative positioning. This method reduced communication and computation costs by using a neural network-based surrogate model as a replacement for the advantage function of the sequential greedy (SG) algorithm. Liao, Su, and Wu [28] proposed a mobile underwater positioning scheme based on reinforcement learning (RL) and neural networks to optimize the selection of anchor nodes in UASNs, achieving precise positioning of targets. These methods can significantly improve the positioning accuracy of UUV clusters through training and prediction. However, they have higher computational complexity, and when individual UUVs in the cluster experience sudden errors, it can affect the overall positioning accuracy of the entire cluster. Neural network-based methods (e.g., BPNN) exhibit high localization accuracy in complex tasks, yet their substantial resource demands significantly limit their applicability in resource-constrained scenarios, such as UUV clusters. The training phase requires extensive offline computational resources and time (e.g., hyperparameter tuning, large-scale data iterations), while online inference introduces considerable latency (milliseconds to seconds) due to forward propagation in multi-layer networks, compromising real-time performance. Additionally, the memory footprint of network weights and intermediate activations (typically ranging from megabytes to gigabytes) poses severe challenges to the storage and power consumption of embedded devices.

To achieve fast positioning of UUV clusters under free aggregation and dispersion conditions, many researchers in the field of wireless network positioning have found that factor graph theory can effectively meet the requirements of UUV clusters. This paper [29] addresses the problem of multitarget tracking using a network of sensing agents with unknown positions. These problems are jointly resolved using a holistic and centralized approach where graph theory is used to describe the statistical relationships among agent states, target states, and observations. A scalable message passing scheme, based on the sum-product algorithm, enables the marginal posterior distributions of both agent and target states to be efficiently approximated. In this tutorial paper [30], we advocate a recently proposed paradigm for scalable multitarget tracking that is based on message passing or, more concretely, the loopy sum-product algorithm. This approach has advantages regarding estimation accuracy, computational complexity, and implementation flexibility. Yan, Luan, and Liu [31] introduced a maximum entropy factor graph (MEFG) algorithm to study the cooperative positioning problem of multiple unmanned underwater vehicles (UUVs). They combined factor graph theory with maximum correlation entropy theory and compared it with traditional positioning algorithms. The validation results showed that the proposed MEFG algorithm achieved significantly lower positioning errors than other algorithms.

Zhang, Wu, and Tang [32] proposed a factor graph-based cooperative positioning method for underwater UUV clusters. This method utilized factor graphs and product theory to establish confidence models for the positioning information of individual UUVs based on range measurements between them, constructing a distributed architecture for underwater UUV cluster cooperative positioning. Although the use of factor graph methods enables fast positioning of UUV clusters and meets their requirements for free aggregation and dispersion, they have a high requirement for time synchronization. Larger time intervals can lead to increased positioning errors, and when individual UUVs experience sudden errors, it can directly impact the overall positioning performance of the entire UUV cluster.

With the development of UUV swarm navigation and positioning, we have discovered that information geometry techniques can effectively address the challenges of processing complex navigation information. Cheng, Wang, and Morelande [33] have explored the relationship between information geometry and the performance of sensor networks in target tracking, aiming to gain a better understanding of deployment, planning, and scheduling issues. Information geometry is utilized to solve problems such as calculating the amount of information collected by sensors in the system and optimizing the scheduling of network sensors and resources. Tang, Wang, and Zhang [34] proposed a UAV cluster cooperative positioning method using information geometry (IGUP) for multi-source fusion. This method transformed various types of navigation source information into information geometry probability models, reducing the impact of random errors. They also introduced the Kullback–Leibler divergence minimization (KLM) fusion method, which enabled fast fusion on geometric manifolds, creatively addressing the fusion challenges arising from different positioning information formats and parameters. Tang, Wang, and Zhang [34] proposed a multi-vehicle three-dimensional cooperative positioning algorithm (MVCP-GW) based on GNSS/wireless base station navigation information geometry probability fusion. They transformed various navigation source information into information geometry probability models, unified the time–frequency parameters of navigation information, and reduced the impact of sudden errors. By combining the Kullback–Leibler algorithm (KLA) fusion method, they broke the limitations of the probability two-dimensional model and achieved multi-vehicle three-dimensional cooperative positioning. Information geometry techniques treat the positioning problem as an optimization problem and utilize geometric relationships and information propagation to solve for the optimal position solution. However, due to the free aggregation and dispersion characteristics of UUVs, changes in the number of UUVs within the cluster can lead to sudden errors in the positioning results of the UUV cluster.

The distributed information fusion strategy, in which the local information is shared among sensors, is one of the key aspects of this intelligent network [35]. Alternative approaches have recently been suggested using distributed stationary and mobile sensors, such as autonomous underwater vehicles (AUVs). In contrast with the use of standard assets, these small, low-power, and mobile devices have limited processing and wireless communication capabilities. However, when deployed in a spatially separated network, these sensors can form an intelligent network achieving high performance with significant features of scalability, robustness, and reliability. Marine robotics is an emerging technological area that enables the development of advanced networks for underwater surveillance applications. When deployed in a region of interest, these robots can cooperatively form an intelligent network achieving high performance with significant features of scalability, adaptability, robustness, persistence, and reliability. Such networks of robots can be the enabling technology for a wide range of applications in the maritime domain. However, this approach [36] is often costly and manpower intensive.

In recent years, scholars have proposed various lightweight localization solutions to address the challenges of limited environmental perception in underwater settings. For instance, dell'Erba [37] (2015) introduced a method for determining the spatial configuration of underwater swarms under minimal data constraints, leveraging optimization algorithms to fuse sparse relative positional information (e.g., angles and distances) for swarm topology reconstruction in low-bandwidth communication scenarios, thereby providing a theoretical framework for resource-constrained environments. However, this method relied on static environmental assumptions and exhibited limited adaptability to dynamic seawater conditions, such as turbidity variations. To address this, dell'Erba [38] further explored non-acoustic ranging techniques, systematically demonstrating the potential of high-power LED in underwater distance estimation in subsequent studies (dell'Erba, 2020, 2021). By establishing correlations between light intensity attenuation models and the optical propagation characteristics of seawater, their work achieved robust ranging in unknown water quality conditions and incorporated dynamic calibration mechanisms to compensate for environmental noise [39]. Experiments demonstrated that LED-based ranging technology could control errors within 1 m in shallow, turbid waters, offering a novel approach to low-cost swarm localization. Nevertheless, existing methods still face challenges such as inefficiency in multi-source heterogeneous data fusion and insufficient real-time performance, particularly in dynamic swarm dispersion–aggregation scenarios.

To address the limitations of the aforementioned UUV cluster positioning methods in meeting the requirements of free aggregation, dispersion, and real-time performance [40], this paper proposes a navigation positioning method for unmanned underwater vehicle (UUV) clusters based on information geometry cooperative fusion. In the following sections, we will provide a detailed explanation of the proposed UUV cluster navigation positioning method based on information geometry cooperative fusion and validate its performance and effectiveness through experiments.

2.2. Theoretical Foundations of Baseline Methods

To provide a rigorous basis for comparative analysis, this subsection details the mathematical formulations of three baseline positioning methods: Recursive Least Squares (RLS), Unscented Kalman Filter (UKF), and Backpropagation Neural Network (BPNN). These methods are widely adopted in underwater positioning research.

2.2.1. Recursive Least Squares (RLS)

The RLS algorithm iteratively minimizes the weighted sum of squared residuals to estimate positional parameters. Let $\mathbf{W}_k \in \mathbb{R}^m$ denote the weight vector at iteration k, $\mathbf{H}_k \in \mathbb{R}^{n\times m}$ the observation matrix, and $\mathbf{z}_k \in \mathbb{R}^n$ the measurement vector. The update rule is the following:

$$\mathbf{W}_{k+1} = \mathbf{W}_k + \gamma \mathbf{P}_k \mathbf{H}_k^T (\mathbf{z}_k - \mathbf{H}_k \mathbf{W}_k) \tag{1}$$

where $\mathbf{P}_\mathrm{k} = (\mathbf{H}_k^T \mathbf{H}_k)^{-1}$ is the inverse covariance matrix, and $y \in (0, 1]$ is the forgetting factor that discounts older data. While RLS offers simplicity, its reliance on sequential updates $\mathcal{O}(m^2)$(complexity per iteration) and sensitivity to abrupt errors (e.g., signal occlusion) limit its robustness in dynamic UUV clusters.

2.2.2. Unscented Kalman Filter (UKF)

The UKF addresses nonlinear state estimation through deterministic sigma-point sampling. For a state vector $\mathbf{x}_k \in \mathbb{R}^n$ and covariance $\mathbf{P}_{\mathrm{k|k}}$, sigma points $X_k^{(i)}$ are selected as follows:

$$X_k^{(i)} = \hat{\boldsymbol{x}}_{k|k} \pm \sqrt{(n+\lambda)\mathbf{P}_{\mathrm{k\,|\,k}}}^{(i)},\ i = 1, \ldots,\ 2n \tag{2}$$

where λ scales the spread of sigma points. These points propagate through nonlinear dynamics, and the posterior mean $\hat{\boldsymbol{x}}_{k+1|k+1}$ and covariance $\mathbf{P}_{k+1|k+1}$ are computed via weighted averaging. Though UKF handles non-Gaussian noise better than the extended Kalman filter (EKF), its $\mathcal{O}(n^3)$ complexity and centralized architecture make it unsuitable for large-scale UUV swarms.

2.2.3. Backpropagation Neural Network (BPNN)

BPNN employs gradient descent to optimize a multi-layer network for position regression. Let $\mathbf{W}_k \in \mathbb{R}^m$ be the true UUV position and $\mathbf{W}_k \in \mathbb{R}^m$ the network output. The loss function combines mean squared error and L2 regularization:

$$\mathcal{L} = \frac{1}{N}\sum_{i=1}^{N} ||\boldsymbol{y}_i - \hat{\boldsymbol{y}}_i||^2 + \lambda ||\mathbf{W}||^2, \tag{3}$$

where $\mathbf{W}$ denotes network weights, and λ controls regularization strength. A typical architecture includes an input layer (e.g., sonar/INS data), two hidden layers with ReLU activation, and a linear output layer. Despite high accuracy, BPNN demands extensive offline training $\mathcal{O}\left(N_{epochs} \cdot N_{data} \cdot N_{weights}\right)$ and significant memory (>10 MB for weights), rendering it impractical for resource-constrained UUVs.

3. System Model

In the framework of this study, we aim to delve into the complexities of cluster cooperative localization by concentrating on UUV clusters as the primary subject of analysis. We have developed a model for a multi-source cooperative localization system tailored to a UUV cluster, illustrated in Figure 1. Within Figure 1, the blue region signifies the maritime zone where the UUV cluster is located. The red connections between UUVs illustrate their capability for mutual distance measurement and communication. The yellow connections denote the ranging and communication links between the UUVs and underwater base stations, highlighting the UUVs' ability to utilize these stations for localization purposes. Moreover, the black dashed lines suggest that the unmanned vehicles are equipped with inertial navigation units, indicating the potential use of inertial navigation systems (INS) by the UUVs for localization.

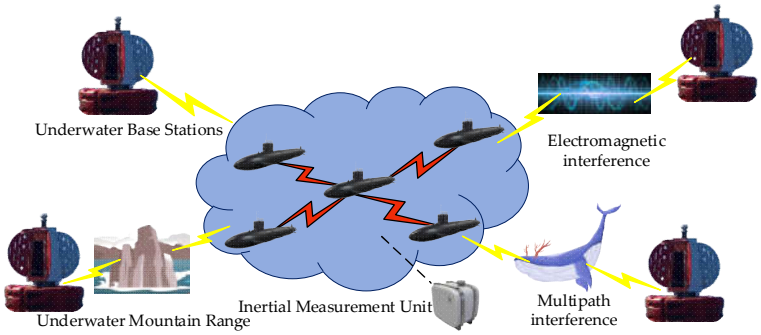


Figure 1. UUV cluster multi-source cooperative localization system model.

The formulation of the information density function aligns with the principles of information geometry, as described in the foundational work by Amari [41]. Specifically, the Kullback–Leibler divergence (KLD)-based fusion criterion (Equation (5)) follows the geometric framework for probabilistic model fusion over statistical manifolds, which unifies heterogeneous sensor data through intrinsic geometric properties [41,42].

Through analysis, the probabilistic information models for the two navigation sources, UBS and INS, can be consistently expressed as follows:

$$\begin{cases} P_{UBS} \sim \mathcal{N}(\boldsymbol{\mu}_{UBS}, \boldsymbol{\Sigma}_{UBS}) \\ P_{INS} \sim \mathcal{N}(\boldsymbol{\mu}_{INS}^{t}, \boldsymbol{\Sigma}_{INS}^{t}) \end{cases} \tag{4}$$

In the Equation (4), $\mathrm{P} \sim \mathcal{N}(\boldsymbol{\mu}, \boldsymbol{\Sigma})$ represents the positioning result of the navigation source as $\boldsymbol{\mu} = [\mathrm{x}, \mathrm{y}, \mathrm{z}]^{\mathrm{T}}$, and the covariance matrix of the positioning result is $\boldsymbol{\Sigma}$. μ serves as the optimal estimate at the current time step. Both $\boldsymbol{\mu}$ and the covariance $\boldsymbol{\Sigma}$ are updated synchronously, but their updates are not directly dependent on each other's changes. Instead, they are collectively governed by the system dynamics model and observational data inputs.

For the target UUV requiring localization, assume there are N available sources of navigation positioning information. The probability density function of the i-th piece of positioning information is denoted by function $p_i(\cdot)$, and its corresponding weight factor in the fusion process is denoted by a_i. The combined information density function is also represented as $p_f(\cdot)$. The fusion criterion used in this section is as follows:

$$p_f = arg\ inf_p \sum_{i=1}^{N} a_i D_{KLD}(p, p_i) \tag{5}$$

In Equation (5), "*arginf*" signifies the point of maximum value for the likelihood function, and $D_{KLD}(p_m, p_i)$ denotes the Kullback–Leibler divergence between the two probability density functions of the information.

$$D_{KLD}(p_m, p_n) = \int p_m In(p_m / p_n) \tag{6}$$

Given that the random error in this section is Gaussian white noise, we can approximately assume that the positioning results $\mathbf{x}$ from various navigation sources follow a three-dimensional Gaussian distribution, with mean $\boldsymbol{\mu} = [\mathrm{x}, \mathrm{y}, \mathrm{z}]^{\mathrm{T}}$ and covariance matrix $\boldsymbol{\Sigma}$. Consequently, the information probability function $\mathrm{p} \sim \mathcal{N}(\boldsymbol{\mu}, \boldsymbol{\Sigma})$ of the navigation source can be represented as follows:

$$\begin{aligned} p(\mathbf{x}|\boldsymbol{\mu}, \boldsymbol{\Sigma}) &= \frac{1}{(2\pi)^{3/2}|\boldsymbol{\Sigma}|^{1/2}} exp\left\{ -\frac{1}{2}(\mathbf{x} - \boldsymbol{\mu})^T \Sigma^{-1} (\mathbf{x} - \boldsymbol{\mu}) \right\} \\ &= exp\left\{ -(1/2)\mathbf{x}^T \boldsymbol{\Sigma}^{-1} x + \left(\boldsymbol{\Sigma}^{-1} \boldsymbol{\mu} \right)^T \mathbf{x} + \zeta \right\} \end{aligned} \tag{7}$$

In Equation (7), ζ is a constant term and is defined as follows:

$$\zeta = -\frac{1}{2}\left(\boldsymbol{\mu}^T \boldsymbol{\Sigma}^{-1} \boldsymbol{\mu} + 3ln(2\pi) + ln|\boldsymbol{\Sigma}| \right) \tag{8}$$

As the positioning information from the navigation sources follows a three-dimensional Gaussian distribution and are independent of each other, solving Equation (5) results in the following:

$$p_f = \frac{\prod_{i=1}^{N} [p_i]^{a_i}}{\int \prod_{i=1}^{N} [p_i]^{a_i}} \tag{9}$$

By inserting Equation (7) into Equation (9), we arrive at the following:

$$p_f\left(\mathbf{x} \middle| \boldsymbol{\mu}_f, \boldsymbol{\Sigma}_f \right) = \frac{\prod_{i=1}^{N} [p_i(\mathbf{x}|\boldsymbol{\mu}_i, \boldsymbol{\Sigma}_i)]^{a_i}}{\int \prod_{i=1}^{N} [p_i(\mathbf{x}|\boldsymbol{\mu}_i, \boldsymbol{\Sigma}_i)]^{a_i}} \tag{10}$$

In Equation (10), $\boldsymbol{\mu}_i$ signifies the positioning result of the i-th navigation source, $\boldsymbol{\Sigma}_i$ indicates the covariance matrix of the i-th navigation source, $\boldsymbol{\mu}_f$ denotes the positioning result after integrating multiple navigation sources, and $\boldsymbol{\Sigma}_f$ refers to the covariance matrix following the fusion of multiple navigation sources. The following relationships apply:

$$\begin{aligned}\prod_{i=1}^{N}[p_i(\mathbf{x}|\boldsymbol{\mu}_i,\boldsymbol{\Sigma}_i)]^{a_i} &= \prod_{i=1}^{N} exp\left\{a_i\left(-(1/2)\mathbf{x}^T\boldsymbol{\Sigma}^{-1}x+\left(\boldsymbol{\Sigma}^{-1}\boldsymbol{\mu}\right)^T\mathbf{x}+\zeta\right)\right\}\\ &= exp\{-(1/2)\mathbf{x}^T(\textstyle\sum_{i=1}^{N}a_i\boldsymbol{\Sigma}_i^{-1})x+\left(\sum_{i=1}^{N}a_i\boldsymbol{\Sigma}_i^{-1}\boldsymbol{\mu}_i\right)^T\mathbf{x}+\sum_{i=1}^{N}a_i\zeta_i\}\end{aligned} \tag{11}$$

By comparing Equations (7) and (11), it is evident that $p_f\left(\mathbf{x}\middle|\boldsymbol{\mu}_f,\boldsymbol{\Sigma}_f\right)$ follows a three-dimensional Gaussian distribution, and we arrive at the following:

$$\begin{cases}\boldsymbol{\Sigma}_f^{-1}=\sum_{i=1}^{N}a_i\boldsymbol{\Sigma}_i^{-1}\\ \boldsymbol{\Sigma}_f^{-1}\boldsymbol{\mu}_f=\sum_{i=1}^{N}a_i\boldsymbol{\Sigma}_i^{-1}\boldsymbol{\mu}_i\end{cases} \tag{12}$$

Solving Equation (12), we can obtain the following:

$$\begin{cases}\boldsymbol{\mu}_f=\left(\sum_{i=1}^{N}a_i\boldsymbol{\Sigma}_i^{-1}\right)^{-1}\left(\sum_{i=1}^{N}a_i\boldsymbol{\Sigma}_i^{-1}\boldsymbol{\mu}_i\right)\\ \boldsymbol{\Sigma}_f=\left(\sum_{i=1}^{N}a_i\boldsymbol{\Sigma}_i^{-1}\right)^{-1}\end{cases} \tag{13}$$

Equation (13) demonstrates that this fusion approach utilizes the weighting factors a_i and the inverses of the covariance matrices $\boldsymbol{\Sigma}_{\mathrm{i}}^{-1}$ to conduct a weighted fusion of the navigation information. This effectively minimizes the impact of navigation sources with significant errors on the fusion outcome.

Information geometry is not merely a mathematical formalism but a principled framework that unifies heterogeneous sensor data geometrically, dynamically balances reliability through intrinsic uncertainty metrics, and outperforms traditional methods in complex underwater scenarios.

In underwater swarm applications, enhancing the collaborative positioning capability of distributed unmanned underwater vehicles, overcoming limitations in information transmission, and addressing challenges posed by environmental variations have emerged as critical issues requiring urgent resolution. To tackle these challenges, this paper proposes an information geometry and factor graph-based collaborative fusion localization method for UUV swarms. The proposed approach transforms individual UUV navigation information into probabilistic models through information geometry, effectively mitigating localization jumps caused by temporal asynchrony among UUVs. Integrated with factor graph theory and inter-UUV ranging measurements, we established a distributed collaborative fusion localization architecture for UUV clusters that enables dynamic cluster formation and dissolution. The implementation framework is illustrated in Figure 2.

As depicted in Figure 2, the architecture comprises two core components: (1) information geometry-based heterogeneous multi-source fusion for individual UUVs and (2) factor graph-based distributed collaborative localization. For each UUV within the cluster, the proposed method first converts positioning information from diverse navigation sources into probabilistic density functions in information geometry space, achieving effective unification of heterogeneous navigation parameter formats to establish a foundation for subsequent fusion. Through information geometry-based multi-source fusion, reliable positioning information for each UUV is generated, serving as the basis for distributed collaborative localization. Leveraging abundant ranging and bearing measurements within the UUV network, we construct a factor graph representation of the swarm, facilitating effective propagation and fusion of localization information among UUVs. This ultimately achieves

distributed collaborative positioning for the entire cluster. The procedural flowchart of the distributed UUV swarm factor graph model is presented in Figure 3.

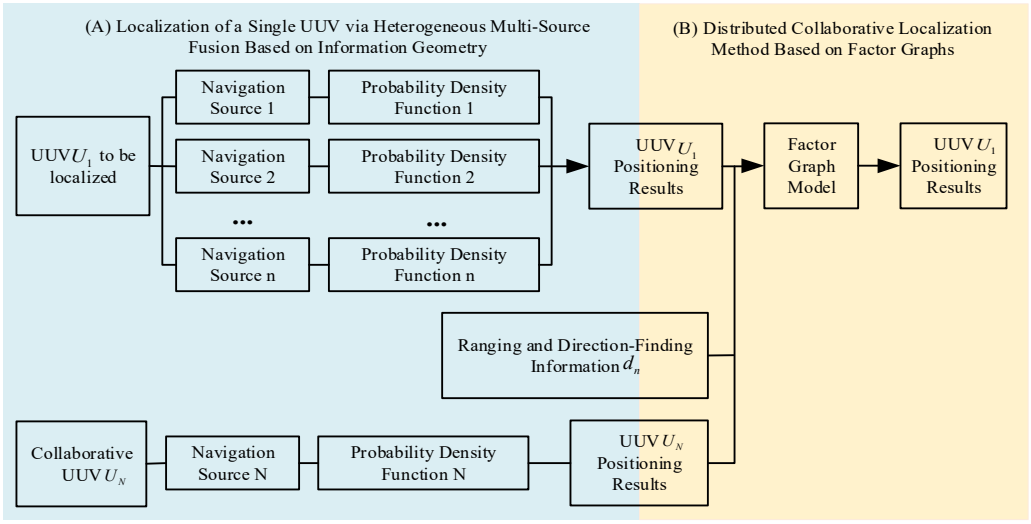


Figure 2. Distributed collaborative localization architecture for UUV swarms with multi-source fusion.

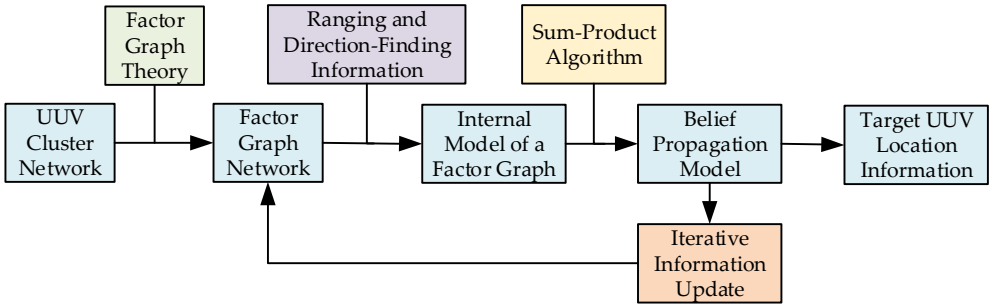


Figure 3. A factor graph-based localization process framework.

As illustrated in Figure 3, the procedural flowchart delineates the distributed UUV swarm factor graph model. First, the factor graph theory is applied to rigorously map the UUV cluster network into a factor graph representation. Subsequently, inter-UUV ranging and bearing measurements are utilized to derive the internal factor graph model for the target UUV. A belief propagation model is then established via the sum-product algorithm, enabling efficient transmission and fusion of localization information among UUVs. Through iterative updates, the collaborative positioning results for the target UUV are ultimately obtained. This distributed cooperative localization framework allows all UUVs within the cluster to perform simultaneous iterative updates, achieving not only swarm-level coordinated positioning but also significantly enhancing overall positioning accuracy and system robustness.

4. Numerical Simulation Setup

Taking any undetermined UUV M_q as an example, suppose the initial position of M_q is $m_q = [x_0, y_0, z_0]^T$. There are n cooperative UUVs surrounding it, with their positions given by $m_i = [x_i, y_i, z_i]^T, i = 1, 2, \cdots n$. Establish a spherical coordinate system using any M_q as the origin, as shown in Figure 4. The distance information from a cooperative UUV M_i to the undetermined UUV M_q can be expressed as $d_i = (r_i, \theta_i, \varphi_i)$, where r_i is the range information, normally distributed with mean r_i and variance $\sigma_{r_i}^2$. The angle φ_i is formed by the semi-plane through the Z-axis and point M_i with the coordinate plane ZOX, and $0 \leq \varphi_i \leq 2\pi$. The angle θ_i is between the line segment M_qM_i and the positive direction of

the Z-axis, with $0 \leq \theta_i \leq \pi$. The positional relationship between the undetermined UUV M_q and cooperative UUV M_i is illustrated in Figure 4.

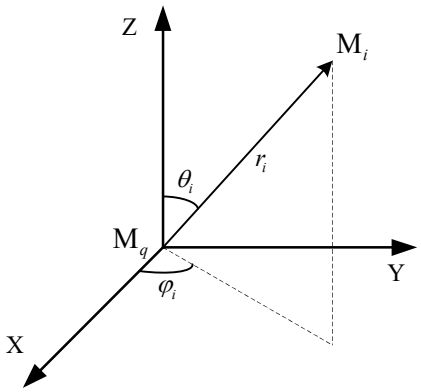


Figure 4. Schematic diagram of the positional relationship.

From the positional relationships in Figure 4, we can obtain the following:

$$\begin{cases} X_i = x + r_i \sin\theta_i \cos\varphi_i \\ Y_i = y + r_i \sin\theta_i \cos\varphi_i \\ Z_i = z + r_i \cos\theta_i \end{cases} \tag{14}$$

Figure 5 presents the internal factor graph model of UUV M_q, which serves as a vital component for multi-source information fusion and cooperative localization within a UUV swarm. By denoting state variables and observational data as variable nodes and function nodes, respectively, this model effectively delineates the interrelationships among various system factors. The message passing employs a bidirectional iterative process based on the sum-product algorithm, where variable nodes first transmit messages to function nodes, followed by function nodes propagating feedback messages back to variable nodes in bottom-up and top-down iterations. This iterative mechanism culminates in an accurate final position estimate for UUV M_q, thereby enhancing localization precision and robustness and establishing a dependable basis for subsequent mission operations.

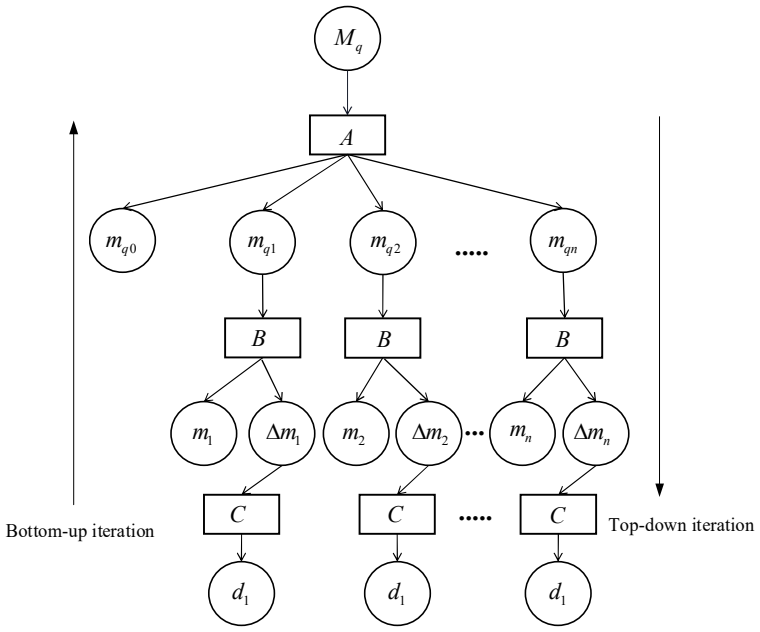


Figure 5. Internal factor graph model.

Figure 5 illustrates the factor graph model developed in this study, wherein component A represents the separation function, component B denotes the error correction function, and component C embodies the iterative function. The initial iterative value is represented as 0, which indicates the starting value of the distance information for iteration. Initially, an initialization procedure is conducted for all UUVs within the network that require localization. Once initialization is finalized, confidence information is exchanged among the UUVs. Considering the k-th iteration as a representative example, the process of information exchange between UUVs and function nodes is delineated as follows.

Initialize all UUVs in the underwater swarm, assuming that the positioning results of the UUVs follow a three-dimensional Gaussian distribution with a mean of $\boldsymbol{\mu} = [\mathrm{x}, \mathrm{y}, \mathrm{z}]^{\mathrm{T}}$ and a covariance of $\boldsymbol{\Sigma}$. The k-th positioning information of the UUV to be positioned $\mathrm{M_q}$ is denoted as $\left(\boldsymbol{\mu}_{\mathrm{q0}}^{\mathrm{k}}, \boldsymbol{\Sigma}_{\mathrm{q0}}^{\mathrm{k}}\right)$, the positioning information of the collaborating UUV $\mathrm{M_i}$ is denoted as $\left(\boldsymbol{\mu}_{\mathrm{i}}^{\mathrm{k}}, \boldsymbol{\Sigma}_{\mathrm{i}}^{\mathrm{k}}\right)$, and the ranging information is $d_{\mathrm{i}}^{\mathrm{k}} = \left(\mathrm{r}_{\mathrm{i}}^{\mathrm{k}}, \theta_{\mathrm{i}}^{\mathrm{k}}, \varphi_{\mathrm{i}}^{\mathrm{k}}\right)$.

To begin, all UUVs within the underwater swarm are initialized under the assumption that their positioning results adhere to a three-dimensional Gaussian distribution characterized by a mean of $\boldsymbol{\mu} = [\mathrm{x}, \mathrm{y}, \mathrm{z}]^{\mathrm{T}}$ and a covariance of $\boldsymbol{\Sigma}$. In this context, the k-th positional data for the target UUV $\mathrm{M_q}$, denoted as $\left(\boldsymbol{\mu}_{\mathrm{q0}}^{\mathrm{k}}, \boldsymbol{\Sigma}_{\mathrm{q0}}^{\mathrm{k}}\right)$, is referred to as $\mathrm{M_i}$, while the positional data for a collaborating UUV is represented as $\left(\boldsymbol{\mu}_{\mathrm{i}}^{\mathrm{k}}, \boldsymbol{\Sigma}_{\mathrm{i}}^{\mathrm{k}}\right)$, accompanied by the ranging information $d_{\mathrm{i}}^{\mathrm{k}} = \left(\mathrm{r}_{\mathrm{i}}^{\mathrm{k}}, \theta_{\mathrm{i}}^{\mathrm{k}}, \varphi_{\mathrm{i}}^{\mathrm{k}}\right)$.

The bottom-up iteration process is initially introduced by entering the factor graph via the function node $\mathrm{C_i}$. Here, the $d_{\mathrm{i}}^{\mathrm{k}} = \left(\mathrm{r}_{\mathrm{i}}^{\mathrm{k}}, \theta_{\mathrm{i}}^{\mathrm{k}}, \varphi_{\mathrm{i}}^{\mathrm{k}}\right)$ information is processed and subsequently transformed into the coordinate difference $\left(\Delta \mathrm{m}_{\mathrm{i}}^{\mathrm{k}}, \boldsymbol{\Sigma}_{\Delta \mathrm{m}_{\mathrm{i}}}^{\mathrm{k}}\right)$, which represents the Euclidean space separation between neighboring UUVs $\mathrm{M_i}$ and $\mathrm{M_q}$.

$$\Delta m_i^k = \left[\Delta x_i^k, \Delta y_i^k, \Delta z_i^k\right]^T = \begin{bmatrix} sin\theta_i^k cos\varphi_i^k \\ sin\theta_i^k sin\varphi_i^k \\ cos\theta_i^k \end{bmatrix} r_i^k \tag{15}$$

$$\boldsymbol{\Sigma}_{\Delta m_i}^k = \begin{bmatrix} sin\theta_i^k cos\varphi_i^k \\ sin\theta_i^k sin\varphi_i^k \\ cos\theta_i^k \end{bmatrix} \sigma_{r_i^{k-1}}^2 \begin{bmatrix} sin\theta_i^k cos\varphi_i^k \\ sin\theta_i^k sin\varphi_i^k \\ cos\theta_i^k \end{bmatrix}^T \tag{16}$$

Then, factor graph is entered through the error correction function $\mathrm{B_i}$ of the ith UUV, the coordinates $\left(\mathrm{m}_{\mathrm{i}}^{\mathrm{k}}, \boldsymbol{\Sigma}_{\mathrm{i}}^{\mathrm{k}}\right)$ of the UUV $\mathrm{M_i}$ and the coordinate difference $\left(\Delta \mathrm{m}_{\mathrm{i}}^{\mathrm{k}}, \boldsymbol{\Sigma}_{\Delta \mathrm{m}_{\mathrm{i}}}^{\mathrm{k}}\right)$ are processed, and the predicted value $\left(m_{qi}^k, \boldsymbol{\Sigma}_{\mathrm{qi}}^{\mathrm{k}}\right)$ of the neighboring UUV $\mathrm{M_i}$ for the UUV $\mathrm{M_q}$ to be located is obtained.

$$m_{qi}^k = m_i^k - \Delta m_i^k \tag{17}$$

$$\boldsymbol{\Sigma}_{q_i}^k = \boldsymbol{\Sigma}_i^k + \boldsymbol{\Sigma}_{\Delta \mu_i}^k \tag{18}$$

Finally, entering the factor graph through the separation function A of the UUV, the predicted value $\left\{ \left(m_{qi}^k, \boldsymbol{\Sigma}_{\mathrm{qi}}^{\mathrm{k}}\right) \middle| \mathrm{i} = 1, 2, \cdots \mathrm{n} \right\}$ and the initial value $\left(m_{q0}^k, \boldsymbol{\Sigma}_{q0}^k\right)$ of the UUV $\mathrm{M_q}$ are fused to obtain the next iteration initial value $\left(\mathrm{m}_{\mathrm{q0}}^{\mathrm{k+1}}, \Sigma_{\mathrm{q0}}^{\mathrm{k+1}}\right)$ of the UUV $\mathrm{M_q}$ to be located. $\sum_{\mathrm{i=0}}^{\mathrm{n}} \Sigma_{\mathrm{m_{qi}^k}}^{-1}$ is the weighted sum of the inverse covariance matrices from multiple sources.

$$m_{q0}^{k+1} = \left(\sum_{i=0}^{n} \boldsymbol{\Sigma}_{m_{qi}^k}^{-1}\right)^{-1} \sum_{i=0}^{n} \left(\boldsymbol{\Sigma}_{m_{qi}^k}^{-1} m_{qi}^k\right) \tag{19}$$

$$\boldsymbol{\Sigma}_{q0}^{k+1} = \left(\sum_{i=0}^{n} \boldsymbol{\Sigma}_{m_{qi}^{k}}^{-1} \right)^{-1} \tag{20}$$

In the top-down iteration, entering the factor graph through the separation function A of the UUV, the confidence information of $(\hat{m}_{qi}^{k}, \boldsymbol{\Sigma}_{\hat{m}_{qi}^{k}}^{k})$ is obtained.

$$\hat{m}_{qi}^{k} = \left(\sum_{j=0, j\neq i}^{n} \boldsymbol{\Sigma}_{m_{qj}^{k}}^{-1} \right)^{-1} \sum_{j=0, j\neq i}^{n} \left(\boldsymbol{\Sigma}_{m_{qj}^{k}}^{-1} m_{qj}^{k} \right) \tag{21}$$

$$\boldsymbol{\Sigma}_{\hat{m}_{qi}}^{k} = \left(\sum_{j=0, j\neq i}^{n} \boldsymbol{\Sigma}_{m_{qj}^{k}}^{-1} \right)^{-1} \tag{22}$$

Then, the function node B_i processes the feedback information $\left(\hat{m}_{qi}^{k}, \boldsymbol{\Sigma}_{\hat{m}_{qi}}^{k} \right)$ and the predicted positioning information $\left(m_{i}^{k}, \boldsymbol{\Sigma}_{i}^{k} \right)$ of the collaborating UUV M_i to obtain the coordinate difference information $\left(\Delta\hat{m}_{i}^{k}, \boldsymbol{\Sigma}_{\Delta\hat{m}_{i}}^{k} \right)$ for the downlink iteration.

$$\Delta\hat{m}_{i}^{k} = m_{i}^{k} - \hat{m}_{qi}^{k} \tag{23}$$

$$\boldsymbol{\Sigma}_{\Delta\hat{m}_{i}^{k}} = \boldsymbol{\Sigma}_{m_{i}^{k}} + \boldsymbol{\Sigma}_{\hat{m}_{qi}^{k}} \tag{24}$$

Finally, entering the factor graph through the iteration function C_i of the i-th UUV, the vector $\Delta\hat{m}_{i}^{k} = \left[\Delta\hat{x}_{i}^{k}, \Delta\hat{y}_{i}^{k}, \Delta\hat{z}_{i}^{k} \right]^{T}$ is processed to convert it into the initial distance information $d_{i}^{k+1} = \left(d_{i}^{k+1}, \theta_{i}^{k+1}, \varphi_{i}^{k+1} \right)$ for the next iteration.

$$r_{i}^{k+1} = r_{i}^{k} \tag{25}$$

$$\theta_{i}^{k+1} = \cos^{-1} \left[\frac{\Delta\hat{z}_{i}^{k}}{\sqrt{\left(\Delta\hat{x}_{i}^{k} \right)^{2} + \left(\Delta\hat{y}_{i}^{k} \right)^{2} + \left(\Delta\hat{z}_{i}^{k} \right)^{2}}} \right] \tag{26}$$

$$\varphi_{i}^{k+1} = \tan^{-1} \left(\frac{\Delta\hat{y}_{i}^{k}}{\Delta\hat{x}_{i}^{k}} \right) \tag{27}$$

$$\sigma_{r_{i}^{k+1}}^{2} = \mathrm{tr} \left(\boldsymbol{\Sigma}_{\Delta\hat{m}_{i}^{k}} \right) \tag{28}$$

In the collaborative positioning method based on factor graphs, first, the coordinate estimation information of M_q from adjacent positioning UUVs is collected. Second, each positioning target provides the probability of information required by the function node for M_q, including distance information and mean and covariance of adjacent UUVs. Finally, the confidence probability of the information is iteratively updated on the factor graph to obtain the best positioning accuracy of the UUV.

Factor graphs serve as a practically indispensable framework for UUV swarm localization, extending beyond theoretical utility to address critical operational demands. Their core strengths include the following: free node management, enabling seamless adaptation to dynamic swarm topologies through autonomous node aggregation/dispersal without system reinitialization; irregular fusion capability, robustly integrating heterogeneous and unreliable data sources (e.g., acoustic ranging, inertial measurements) via probabilistic consistency constraints; real-time scalability, achieving O(N) computational complexity and bandwidth-efficient communication through localized message passing.

This architecture ensures resilient performance in GPS-denied environments while maintaining sub-meter accuracy under dynamic node changes and data heterogeneity, as validated in field trials with six UUVs.

Overall Algorithm Implementation Steps

The proposed factor graph-based cooperative localization method for unmanned underwater vehicle (UUV) clusters is implemented through the steps illustrated in Figure 6.

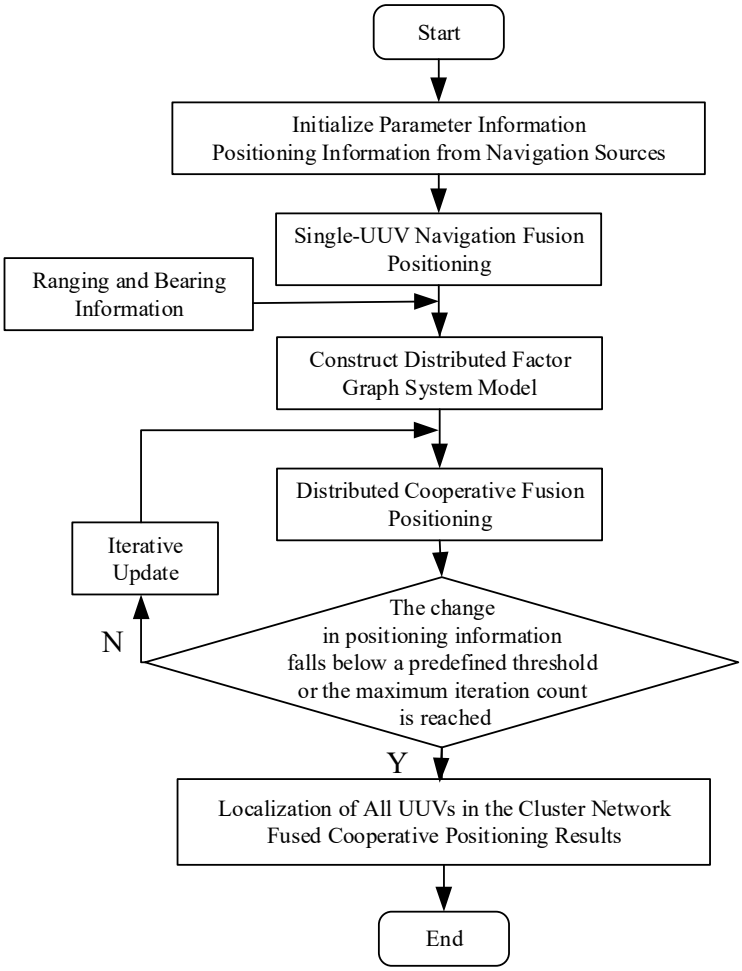


Figure 6. UCDFP method flowchart.

As shown in Figure 6, the algorithm implementation process consists of several key steps. First, positioning information from various navigation sources is acquired to establish the foundational data for subsequent steps. Next, through information probability modeling and fusion criteria based on information geometry theory, the navigation source positioning data are processed to generate single-UUV multi-source fused localization results. The most critical step involves constructing a distributed cooperative localization factor graph model using inter-UUV ranging and bearing measurements. This model enables effective propagation and fusion of positioning information among UUVs, achieving cluster-level cooperative localization.

Subsequently, the algorithm employs the sum-product algorithm for iterative message passing. Specifically, the information propagation is divided into two phases: an upward process, where variable nodes transmit state information to function nodes, and a downward process, function nodes compute feedback based on received states and propagate results back to variable nodes.

This process iterates until convergence criteria are met (e.g., information changes fall below a predefined threshold, or the maximum iteration count is reached). Finally, the algorithm calculates the fused cooperative positioning results for all UUVs in the cluster network based on the iteratively updated belief model.

5. Testing and Results Analysis

This paper will validate the performance of the unmanned underwater vehicle cluster navigation information geometric collaborative fusion positioning (UCDFP) method in terms of positioning accuracy, convergence speed, and free clustering and dispersing capability. The performance will be compared with the Recursive Least Squares method (RLS) proposed in the literature, the Unscented Kalman Filter method (UKF) proposed in the literature, and the artificial neural network method (ANN) proposed in the literature. The simulation experiments consist of two parts: the first part is an ideal scenario where no navigation source signals are lost, which mainly analyzes the impact of key parameters on the accuracy of fusion collaborative positioning and convergence speed; the second part is a sudden-change scenario where some navigation source signals are subject to interference or even interruption, to verify the stability of the UCDFP method. When evaluating the positioning accuracy, this section uses the root-mean-squared error (RMSE) to reflect the positioning accuracy. RMSE is a commonly used metric for measuring the difference between predicted values and true values, and a smaller RMSE indicates higher predictive accuracy of the model.

5.1. Simulation Condition Settings

In the information geometry collaborative fusion method proposed for UUV cluster navigation in this paper, UUVs achieve positioning by exchanging information with other UUVs within communication range. The simulation environment is a collaborative positioning network area of 100 × 100 × 50 m, containing 50 UUVs that move at a constant speed of 3 m/s in random directions. After multiple rounds of simulation debugging, the standard deviation of the ranging error of each UUV is set to 2 m, and the position ambiguity σ_p is set to 2 m.

The simulation parameters of this paper are shown in Table 1. To ensure ranging accuracy, communication and ranging between UUVs within the collaborative network area are in a fully connected state. UUVs are randomly distributed in three-dimensional space, and the network topology is shown in Figure 7. In the figure, blue solid circles represent UUVs, and communication between UUVs is indicated by green lines.

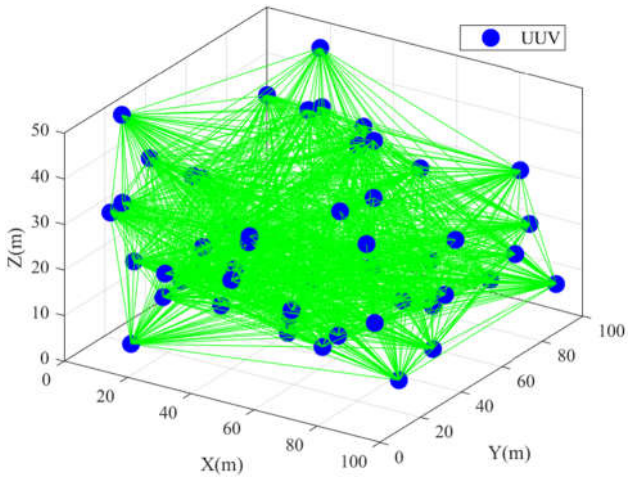


Figure 7. UUV cluster network topology diagram.

Table 1. Simulation parameter settings of underwater base station.

Simulation Parameters	Parameter Settings
Number of underwater base stations	$n = 8$
Underwater base station locations	Vertices of the simulation scenario
Standard deviation of underwater ranging error	$\sigma_2 = 2$ m
Inertial navigation parameters	Consistent with Table 2
Minimum output time interval	0.1 s
Number of Monte Carlo runs	10,000

Table 2. Simulation parameter settings of INS.

Inertial Unit Parameters	Accelerometer	Gyroscope
Bias	$b_a = 1500\mu g$	$b_\omega = 1^\circ/h$
Random error standard deviation	$\sigma_a = 100\mu g/\sqrt{HZ}$	$\sigma_\omega = 0.1^\circ/\sqrt{h}$
Output rate	$f_a = 100$ HZ	$f_\omega = 100$ HZ
Calibration period	$T = 10$ s	

5.2. Ideal Scenario

To further evaluate the positioning performance of the information geometry-based collaborative fusion positioning algorithm for unmanned underwater vehicles, this paper compares the proposed algorithm with the Recursive Least Squares method (RLS), Unscented Kalman Filter method (UKF), and Backpropagation Neural Network method (BPNN) under ideal scenarios. This comparison helps us gain a comprehensive understanding of the performance differences among different algorithms under the same conditions, thereby verifying the effectiveness and superiority of the proposed algorithm. In this simulation, we set the simulation parameters to be the same as those in Section 5.1, involving 50 unmanned underwater vehicles in the collaborative positioning task. During the simulation, each algorithm implementation follows the same initial conditions and iterative process. The average positioning error is selected as the output for comparative analysis, as shown in Figure 8.

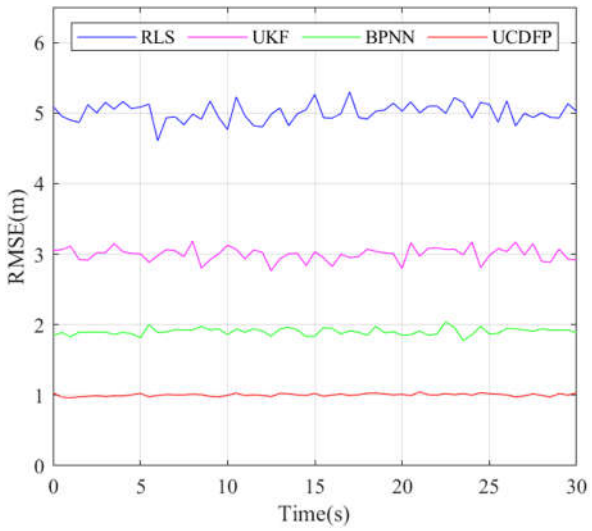


Figure 8. Comparison of positioning errors of four positioning algorithms in an ideal scenario.

As shown in Figure 8, when comparing the information geometry-based collaborative fusion positioning algorithm for unmanned underwater vehicles with other algorithms, we find that the UCDFP method performs the best in terms of average positioning error, with

an average error of only 0.982 m. This result is significantly better than other mainstream algorithms, including the Recursive Least Squares (RLS) method, the Unscented Kalman Filter (UKF) method, and the Back Propagation Neural Network (BPNN) method. This indicates that the information geometry-based algorithm has a distinct advantage in handling measurement errors and position uncertainty in underwater environments. Specifically, the BPNN method has an average positioning error of 1.902 m, second only to the information geometry-based algorithm, demonstrating its effectiveness in certain situations but still unable to match the accuracy of the information geometry algorithm. In contrast, the UKF method has an average positioning error of 3.092 m, showing relatively weak performance, especially in complex underwater environments where it may be affected by noise and dynamic changes. Lastly, the RLS method has an average positioning error of 4.992 m, revealing its inadequacy in positioning accuracy, particularly in underwater environments where it might struggle to meet high-precision positioning requirements.

From Figure 9, it is evident that there are significant differences in convergence speed and positioning accuracy among various localization methods. Specifically, the Recursive Least Squares (RLS) method requires 10 iterations to reach convergence during cooperative localization, but the final convergence error is approximately 4.8 m, indicating relatively low positioning accuracy. In contrast, the Back Propagation Neural Network (BPNN) method has the slowest convergence speed, needing 20 iterations to converge. Although its convergence error improves to about 1.8 m, it still does not meet high-precision positioning requirements. Further analysis shows that the Unscented Kalman Filter (UKF) method converges faster than BPNN, generally achieving convergence after around 15 iterations; however, its convergence error remains about 2.75 m, displaying inadequacy in positioning accuracy. In contrast, the UCDFP method proposed in this paper demonstrates clear advantages in localization performance. This method can achieve convergence after only 10 iterations, and the final positioning error is about 0.972 m, showcasing its superior accuracy. The poor positioning accuracy of the LS method is attributed to its disregard for prior information, leading to error accumulation from the position ambiguity of the UUVs (unmanned underwater vehicles) during iterative updates. Although UCCP and BPNN show significant improvements in positioning accuracy compared to the RLS method, their high computational complexity results in slower convergence speeds. In summary, the UCDFP method exhibits the best positioning accuracy and the fastest convergence speed among the compared methods, effectively meeting the cooperative localization needs of UUV swarms under low-rate communication conditions.

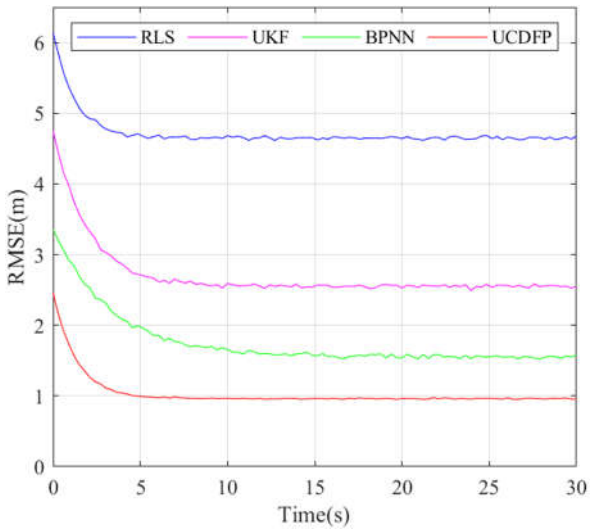


Figure 9. Performance comparison of four positioning algorithms.

In the scenario of cooperative localization for UUV swarms, in addition to ranging errors, the scale of the localization swarm is also an important factor affecting the accuracy of cooperative localization. To further investigate this issue, this paper simulates localization swarms of different scales by varying the number of UUVs. The number of UUVs is set from 2 to 50, with their initial positions randomly distributed within the simulation environment. This random distribution more realistically simulates the deployment of UUVs in practical applications. During the simulation, aside from the change in the number of UUVs, other simulation conditions remain consistent with those in Section 5.1. After conducting the simulation experiments, we obtained results showing how localization accuracy varies with the number of UUVs, which are presented in Figure 10.

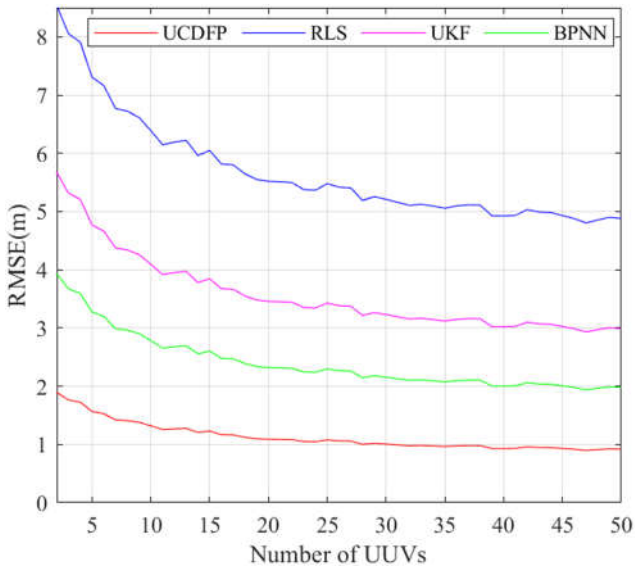


Figure 10. Simulation results of positioning accuracy with varying number of UUVs.

Figure 10 clearly illustrates the trend in localization accuracy as the number of UUVs increases. Generally, with an increase in the number of UUVs, the cooperative localization accuracy of the swarm is improved. This is because more UUVs provide additional ranging information, which enhances the overall reliability and accuracy of localization. However, beyond a certain number, increasing the UUV count may lead to a slowdown in the improvement of localization accuracy or even a saturation effect. This phenomenon may be related to factors such as the network structure of the system, communication delay, and the efficiency of data fusion algorithms. Therefore, when analyzing the simulation results, we should not only focus on improvements in localization accuracy but also consider the reasonableness of swarm size and the overall performance of the system. By comparatively analyzing the localization accuracy of these four methods, it can be observed that under a certain number of UUVs, the UCDFP method's localization accuracy is significantly better than the other three methods. The core reason for this result is that the UCDFP method employs a strategy of constructing a factor graph model for localization, thereby transforming the swarm cooperative localization problem into a distributed cooperative localization problem. In conclusion, the UCDFP method outperforms other methods in UUV swarm cooperative localization, mainly due to its developed factor graph model and distributed information transmission mechanism. Specifically, the performance of the free polydispersion of UUV groups is compared in Table 3.

Table 3. Performance comparison of UUV swarm free aggregation/dispersion.

Method	Average Positioning Error (m)	Error Increment During Dynamic Swarm Changes (m)
UCDFP	0.982	0.3
RLS	4.992	4.8
UKF	3.092	2.75
BPNN	1.902	1.8

During the actual underwater operations of unmanned underwater vehicles (UUVs), changes in environmental factors and mission requirements cause the positions of UUVs to change constantly. This dynamic alteration results in the UUV swarm network exhibiting characteristics of free gathering and dispersing. In terms of localization, this characteristic is reflected in the fluctuation of the number of UUVs participating in localization fusion. To simulate this process, we designed an experiment where we periodically adjust the number of UUVs involved in localization to observe its impact on localization accuracy and convergence speed. Specifically, we set the number of UUVs participating in fusion to change every 20 s interval: from 0 to 20 s, there are 50 UUVs; from 20 to 40 s, the number reduces to 20; from 40 to 60 s, it further decreases to 10; from 60 to 80 s, the number increases back to 30; and finally, from 80 to 100 s, it rises again to 50. This change in numbers simulates the gathering and regrouping phenomena that may occur during UUV tasks due to varying mission needs and environmental conditions. Moreover, other simulation environment parameters remain consistent with those in Section 5.1 to ensure the comparability and validity of the experiment. With these settings, we can comprehensively evaluate the localization performance of UUV swarms with different numbers of participants. The simulation results are shown in Figure 11.

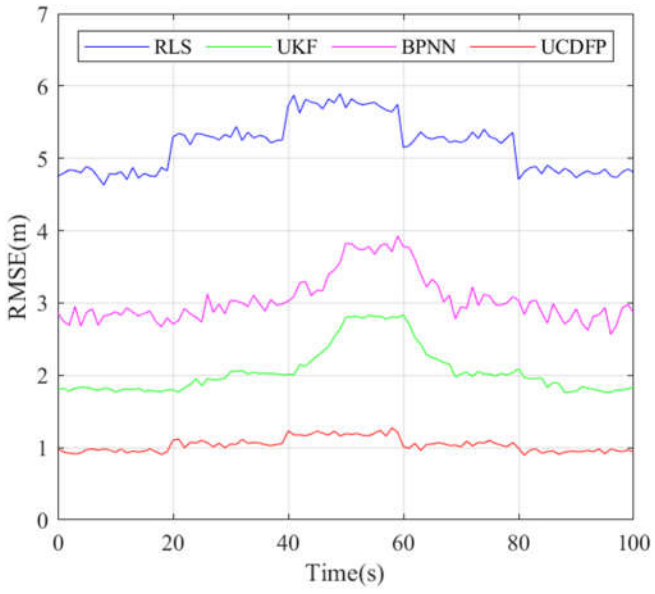


Figure 11. Evaluation of free gathering and dispersing characteristics of a UUV swarm under four methods.

As depicted in Figure 11, during the real-world underwater operations of unmanned underwater vehicles (UUVs), the localization error of the UUV swarm undergoes significant variations in correspondence with the periodic changes in the number of units within the swarm. Specifically, the UCDFP (unmanned cluster dynamic fusion positioning) method proposed in this study showcases remarkably superior performance in managing these

variations. The amplitude of change in the localization error for the UCDFP method is the smallest, measuring approximately only 0.3 m. This result highlights the capability of the UCDFP method to maintain a relatively stable level of localization accuracy across UUV swarms of different sizes. In stark contrast, the other three methods evaluated, namely, the Recursive Least Squares (RLS), Unscented Kalman Filter (UKF), and Back Propagation Neural Network (BPNN) methods, exhibit relatively larger changes in localization error. When these methods are confronted with variations in swarm size, the extent of fluctuation in their localization errors is notably higher compared to the UCDFP method. This suggests that the UCDFP method is not only more robust but also more reliable in preserving localization accuracy amid dynamic changes in UUV swarm sizes, making it a more effective approach for UUV operations that involve variable swarm configurations. The results are shown in Table 4. The ability of UCDFP to deliver consistent performance regardless of the swarm scale underscores its potential as a highly preferred technique in the field, as it ensures precise navigation and operation in diverse scenarios.

Table 4. Performance under sudden-change scenarios.

Method	Convergence Time After Sudden Error (s)	Error Increment During Sudden Changes (m)
UCDFP	1.5	0.352
RLS	2	4.8
UKF	3	2.75
BPNN	5	1.8

5.3. Sudden-Change Scenarios

In complex underwater environments, factors such as ocean reefs and marine life can cause communication signals between UUVs to face obstruction and interference. This can lead to anomalies in ranging information and positioning signals, including sudden changes and signal loss, significantly affecting the accuracy of UUV cooperative positioning. Therefore, this subsection will explore simulation experiments on multi-navigation-source fusion positioning in scenarios with sudden changes.

Subsequently, we will compare the performance of four multi-source fusion positioning methods, RLS, UKF, BPNN, and UCDFP, under sudden-change scenarios to verify the advantages of the UCDFP method in the field of UUV positioning. The setup involves adjusting the pseudo-range error standard deviation, r1, from 1.0 m to 1.5 m during the time interval t = 3~7 s; the underwater base station ranging error standard deviation, r2, changes from 1.0 m to 2.0 m during t = 13~17 s; and the inter-UUV ranging error standard deviation, r3, changes from 1.0 m to 2.0 m during t = 23~27 s. Other parameter settings remain consistent with the ideal scenario. This experiment uses the average positioning error of 50 UUVs as the output metric. The simulation results for the accuracy comparison of multi-source fusion positioning methods under sudden-change scenarios are shown in Figure 12.

As shown in Figure 12, the simulation results indicate that when interference is introduced to the entire UUV cluster during time intervals t = 3~7 s, t = 13~17 s, and t = 23~27 s, the error for all four positioning methods increases. However, the UCDFP method proposed in this paper demonstrates a significant advantage in terms of error increment, exhibiting the smallest increase in error. This method achieves rapid convergence for multi-UUV cooperative positioning within just 2 s. In contrast, the other three methods require considerably more time to return to a stable state when facing the same interference, typically needing 6 to 10 time steps (i.e., 3 to 5 s) to reconverge. This phenomenon suggests that the UCDFP method not only has a faster convergence speed but also shows strong suppression capability against sudden error variations. In summary, the UCDFP method

effectively reduces positioning error and accelerates recovery speed in complex underwater environments, especially under interference, demonstrating its potential advantage in practical applications.

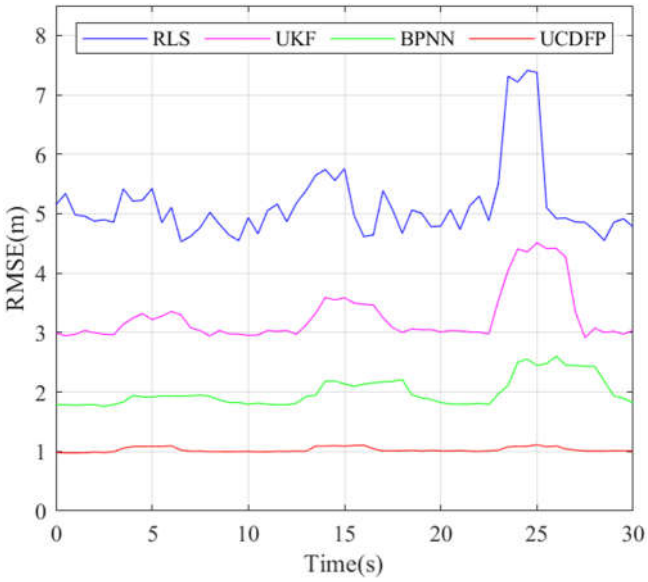


Figure 12. Simulation results of accuracy comparison for multi-source fusion positioning methods under sudden-change scenarios.

6. Experimental Validation and Results Analysis

To validate the effectiveness of the unmanned underwater vehicle cluster navigation information geometric cooperative fusion positioning (UCDFP) method, this paper first designed the method and conducted pool experiments on a verification platform constructed in a laboratory. Figure 13 shows the actual experimental environment. The field experiments were performed in Qixiang Lake (34.1378° N, 108.6594° E) at Northwestern Polytechnical University's Chang'an Campus, with an effective testing area of 120 m × 80 m and an average depth of 10 m (max 15 m). The unmanned underwater vehicles are shown in Figure 14. In the experiment, the unmanned underwater vehicles used were equipped with various sensors, including sonar and inertial measurement units (IMUs), among others, and underwater base station positioning points were set up in the pool. These sensors and base stations provided a wealth of multi-source information. The fusion of this information aims to improve positioning accuracy and reliability. Furthermore, the specific parameter information is shown in Table 5.

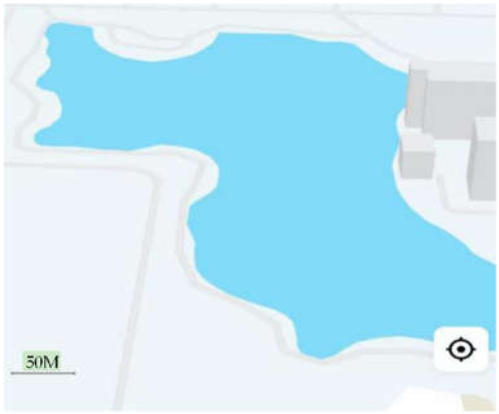


Figure 13. The actual experimental environment.



Figure 14. Example of one of the unmanned underwater vehicles.

Table 5. Specific parameter information is displayed.

Relevant Parameters	Simulation Parameters	Parameter Settings
Inertial Measurement Unit (IMU)	Model	ADIS16470 (Analog Devices) Shenzhen, China
	Accelerometer	Bias stability = 1500 μg Noise density = 100 μg/Hz
	Gyroscope	Bias stability = 1°/h Noise density = 0.1°/$\sqrt{h}$
Acoustic Ranging Sensors	Model	Tritech MicronNav
	Range	0.1–100 m
	Accuracy	±0.1 m (in still water)
	Frequency	25–50 kHz
Underwater Base Stations (UBSs)	Positioning accuracy	±0.5 m (static), ±1.2 m (dynamic)
	Communication	Acoustic modem (WHOI Micro-Modem)
	Bandwidth	4 kHz
Environmental Conditions	Water Properties	Temperature: 10–15 °C; salinity: 35 ppt
	Sound Speed	1500 m/s (calculated using Mackenzie's formula)
	Disturbances	Simulated current speed: 0.5–1.0 m/s (random direction); turbidity: 1–5 NTUs (Nephelometric Turbidity Units)
Communication Protocols	Inter-UUV communication	Time-division multiple access (TDMA)
	Data rate	500 bps (acoustic),
	Packet loss rate	<5% (ideal scenario) <20% (sudden-change scenario)
Experimental Hardware	UUV Platform	Custom-built AUV with 6-DOF thrusters
	Onboard computer unit	NVIDIA Jetson AGX Xavier
	Location	Qixiang Lake (34.1378° N, 108.6594° E)
	Depth	10–15 m
	Test duration	2 h per trial

Actual Testing Scenario

In the actual testing scenario, we deployed six unmanned underwater vehicles (UUVs) and randomly distributed their initial positions within a designated experimental area. Each UUV moved at a constant speed in a straight line throughout the experiment, with the direction of movement being random. This setup aims to simulate various navigational conditions that may be encountered in real-world environments and to evaluate the performance of the positioning system under dynamic conditions. Specifically, we focus on the system's real-time positioning accuracy under uncertain motion patterns. After testing, the results of the positioning trajectories obtained are shown in Figure 15. Such an experimental design provides reliable data support for analyzing the stability and accuracy of the positioning system.

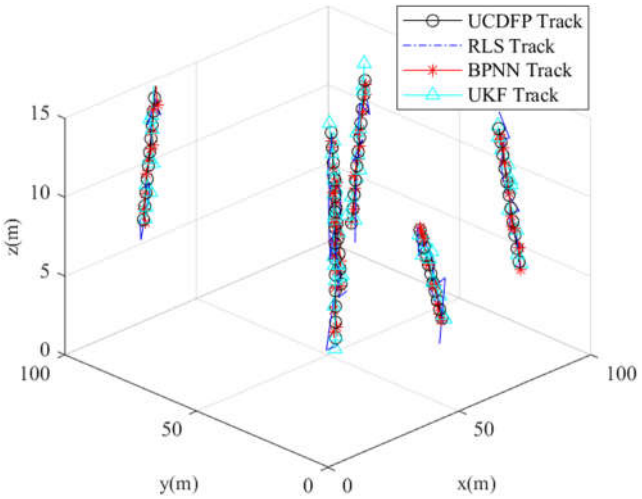


Figure 15. Trajectory results of cooperative positioning for six UUVs.

In Figure 15, the symbol "o" is used to represent the positioning results obtained using our method. Upon examination of the data presented, it becomes clear that the positioning outcomes for the unmanned underwater vehicle (UUV) that employs the UCDFP method are in close proximity to the actual values, indicating high accuracy. To further substantiate the effectiveness and reliability of the UCDFP method, we conducted a comparative analysis with other well-established methods, namely the Recursive Least Squares (RLS) method, the Unscented Kalman Filter (UKF), and the Back Propagation Neural Network (BPNN) method. Figures 5–15 illustrate the positioning errors observed for the UUV when different positioning methods are utilized. The figures demonstrate that, in the absence of sudden error fluctuations, the RLS and UKF methods exhibit the largest positioning errors, indicating significant deviations from the true values. The BPNN method shows intermediate levels of error. In contrast, the UCDFP method consistently demonstrates the smallest positioning errors among all the methods evaluated. This outcome clearly indicates that, compared to the other three methods, the UCDFP method provides significantly higher positioning accuracy under normal operational conditions. Such a performance advantage highlights the potential of the UCDFP method as a superior choice for precise and reliable positioning in underwater navigation applications.

This section will provide a systematic performance comparison of four positioning methods, specifically including the Recursive Least Squares (RLS) method, Unscented Kalman Filter (UKF), Back Propagation Neural Networks (BPNNs), and the unmanned underwater vehicle cooperative fusion positioning method based on information geometry (UCDFP). To ensure the reliability and validity of the comparison results, we conducted experiments in a real-world pool environment, with the experimental results shown in

Figure 16. During the experiments, we assessed the positioning accuracy and robustness of these four methods under different interference conditions. The goal was to gain a comprehensive understanding of the performance of each method.

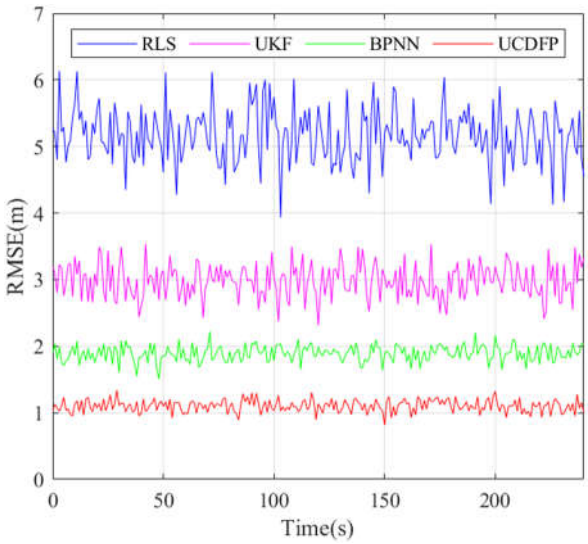


Figure 16. Actual experimental validation results diagram.

During real-world operations of unmanned underwater vehicle (UUV) swarms, environmental factors such as water currents, temperature variations, and acoustic interference can disrupt navigation sources and degrade communication links between UUVs. These disruptions may result in communication failures or signal attenuation, leading to sudden positioning errors. Such errors not only compromise the localization accuracy of individual UUVs but also undermine the collaborative efficiency of the entire swarm. To address these challenges, rigorous research into localization methods under sudden disturbance scenarios is essential. This subsection evaluates the robustness of the UCDFP method in dynamic environments with abrupt disturbances through systematic simulation experiments. To ensure the generalizability of findings, simulations incorporate controlled scenarios with unexpected error injections to replicate real-world signal instability.

In the real-world test scenario, we deployed six UUVs and randomly distributed their initial positions within a designated experimental area. Each UUV had varying speeds throughout the experiment, and their movement directions were random. This setup is designed to simulate various navigation conditions that might be encountered in real environments, thereby evaluating the positioning system's performance under dynamic conditions. Specifically, we focused on the system's real-time positioning accuracy under uncertain motion patterns. After testing, we obtained the positioning trajectory results shown in Figure 17.

To thoroughly investigate the sudden error suppression capability of the UCDFP method in complex underwater environments, a series of experiments was designed based on the actual test verification experiment. These experiments introduced artificial disturbances to simulate potential sudden errors that might occur in real environments. The purpose of this process is to evaluate the robustness and adaptability of the UCDFP method when faced with unexpected disturbances. During the experiments, sudden errors were introduced at the positioning time of t = 110~130 s. These errors might arise from changes in water currents, equipment malfunctions, or other external factors. For this purpose, we selected six UUVs that participated in the actual test, recording their average positioning errors after the introduction of sudden errors, which served as the output metric for analysis. The experimental results are presented in Figure 17.

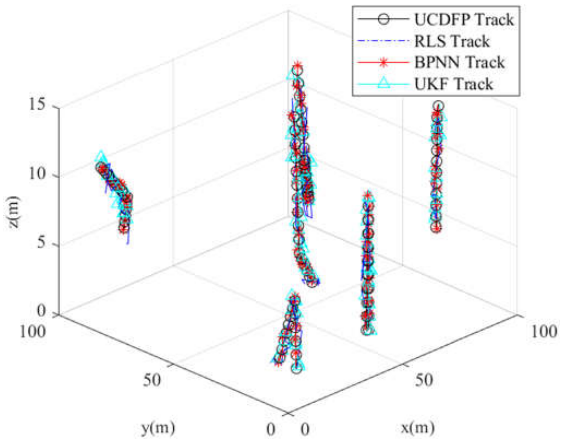


Figure 17. Actual test verification experiment positioning trajectory results.

As shown in Figure 18, under conditions where ranging suddenly changes, the UCDFP method still maintains the highest positioning accuracy. Specifically, when the sudden change occurs, the average error increment of the UCDFP method is only 0.352 m, demonstrating its superior performance in handling sudden errors. By constructing a distributed factor graph model, UCDFP can effectively integrate positional information from different UUVs, significantly reducing the impact of sudden errors on the positioning accuracy of the vehicle cluster, thereby showcasing excellent error suppression capabilities. Compared to the other three methods (RLS, BPNN, and UKF), UCDFP not only excels in positioning accuracy but also has a clear advantage in convergence speed. This means that in the event of sudden changes in ranging, UCDFP can quickly adapt to the changes and promptly adjust the positioning strategy, effectively suppressing the impact of sudden changes on positioning accuracy. During the experiment, we observed that other methods showed relatively larger error increments and slower convergence speeds after the sudden change, extending the recovery time for positioning accuracy. This significant difference mainly arises from the unique information processing advantages of the UCDFP method. Utilizing the theory of information geometry, UCDFP better handles uncertainties and sudden factors, ensuring efficient positioning performance in dynamic environments. This characteristic endows UCDFP with stronger adaptability and practicality in real-world applications, especially in complex and unstable underwater environments. In conclusion, when dealing with sudden changes in ranging, the UCDFP method not only maintains higher positioning accuracy but also quickly adapts to and suppresses the impact of sudden changes on positioning accuracy.

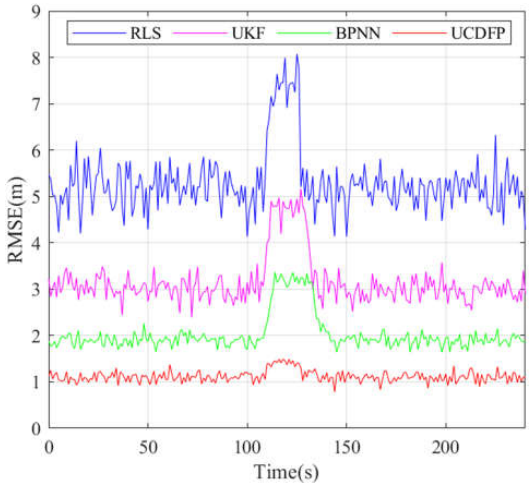


Figure 18. Results of the actual sudden-change experiment.

7. Conclusions

This paper proposes an information geometry-based cooperative fusion positioning method for unmanned underwater vehicle (UUV) clusters. First, a mathematical model for a single-vehicle multi-source positioning system is theoretically constructed, clarifying the characteristics of underwater base stations and inertial navigation and their roles in the positioning process. Then, the various navigation sources are analyzed to derive probabilistic models for two common navigation sources, achieving a unified format for heterogeneous navigation source parameter information. Next, the navigation information of each UUV is converted into information geometric probabilistic models, effectively reducing the impact of time asynchrony on positioning. Based on factor graph theory and ranging information between UUVs, the authors constructed a distributed UUV cluster cooperative fusion positioning architecture, realizing free fusion and dispersion among UUV clusters. Finally, through simulation experiments and empirical validation, the proposed method (UCDFP) was compared with the Recursive Least Squares (RLS), Backpropagation Neural Network (BPNN), and Unscented Kalman Filter (UKF) methods. The results show that the proposed method excels in convergence speed and the UUV cluster's free aggregation and dispersion capabilities. The experimental results demonstrate that the method is efficient and feasible in practical applications, significantly outperforming traditional positioning methods in terms of positioning accuracy, stability, and anti-interference capability, fully showcasing its advantages in complex environments.

Looking forward, this method can be further expanded and improved. While the proposed information geometry and factor graph-based collaborative localization method for UUV swarms demonstrates significant advantages in dynamic environment adaptation and heterogeneous data fusion, several limitations warrant further investigation. The computational complexity, though linear $O(N)$, may still incur latency in large-scale clusters $N > 50$, particularly during rapid node reconfiguration or swarm expansion, necessitating lightweight hierarchical fusion architectures with edge-assisted pre-processing. The method's reliance on Gaussian assumptions for sensor noise and environmental disturbances becomes inadequate under extreme nonlinear interference (e.g., heavy-tailed acoustic errors in turbulent flows or sensor failures), calling for robust nonparametric models like Dirichlet process mixtures integrated with anomaly detection. Dynamic swarm topologies introduce transient errors during frequent node exit events, which could be mitigated via incremental manifold learning and distributed consensus protocols. Communication constraints in low-bandwidth underwater channels risk information loss during covariance matrix transmission, prompting the need for compressed sensing and error-correcting codes (e.g., fountain codes). Additionally, current validation in controlled lake environments overlooks deep-sea challenges (e.g., high pressure, magnetic interference), underscoring the importance of multi-region collaborative trials. Future work will focus on reinforcement learning-driven adaptive fusion, edge–cloud hybrid architectures for scalability, and physics-informed models incorporating fluid dynamics to enhance prediction consistency. These advancements aim to bridge the gap between theoretical innovation and real-world deployment in complex marine operations.

The potential applications and future extensions of the UCDFP method are highly enlightening, specifically reflected in the following three directions: Firstly, in the field of marine resource exploration, it provides technical support for the 3D modeling and sampling path planning of deep-sea polymetallic nodules. Secondly, in underwater infrastructure monitoring, UCDFP dynamically adjusts the topology of UUV swarms to maintain sub-meter positioning accuracy in the presence of strong current disturbances, thereby enhancing the efficiency of underwater pipeline inspections. Finally, in the biomedical field, through FPGA acceleration and the miniaturization improvements of the lightweight

factor graph model, UCDFP can be adapted for in vivo targeted drug delivery tasks using micro-medical robot swarms.

In conclusion, the information geometry-based cooperative fusion positioning method for UUV clusters proposed in this paper provides an effective solution to the positioning problem of unmanned underwater vehicle clusters. This method has potential applications in improving positioning accuracy, stability, and cluster cooperative capabilities and offers valuable references for further research in the field of unmanned underwater vehicles. The distributed, low-complexity nature of UCDFP makes it possible to be applied to other group systems with similar resource limitations (such as drones and Internet of Things networks).

Author Contributions: Conceptualization, C.T.; Software, S.W.; Formal analysis, H.L.; Data curation, L.Z.; Writing—original draft, L.Z.; Supervision, C.T. All authors have read and agreed to the published version of the manuscript.

Funding: This research was funded by Natural Science Foundation of China grant number 62171375, 62271397, 62173276, 62101458, 62001392, 61803310, and 61801394, and the Shenzhen Science and Technology Program grant number JCYJ20220530161615033.

Data Availability Statement: The data presented in this study are available on request from the corresponding author. Due to the need for relevant data in later research, the data can only be provided separately upon application by relevant personnel.

Acknowledgments: The authors would like to thank the editors for their rigorous work and the anonymous reviewers for their comments and suggestions.

Conflicts of Interest: The authors declare no conflict of interest.

References

1. Yuan, S.; Li, Y.; Bao, F.; Xu, H.; Yang, Y.; Yan, Q.; Zhong, S.; Yin, H.; Xu, J.; Huang, Z.; et al. Marine environmental monitoring with unmanned vehicle platforms: Present applications and future prospects. *Sci. Total. Environ.* **2022**, *858*, 159741. [CrossRef] [PubMed]
2. Wang, X.; Shang, J.; Luo, Z.; Tang, L.; Zhang, X.; Li, J. Reviews of power systems and environmental energy conversion for unmanned underwater vehicles. *Renew. Sustain. Energy Rev.* **2012**, *16*, 1958–1970. [CrossRef]
3. Bogue, R. Underwater robots: A review of technologies and applications. *Ind. Robot. Int. J.* **2015**, *42*, 186–191.
4. Bai, G.; Chen, Y.; Hu, X.; Shi, Y.; Jiang, W.; Zhang, X. Multi-AUV dynamic trajectory optimization and collaborative search combined with task urgency and energy consumption scheduling in 3-D underwater environment with random ocean currents and uncertain obstacles. *Ocean Eng.* **2023**, *275*, 113841. [CrossRef]
5. Du, Z.; Chai, H.; Xiang, M.; Zhang, F.; Wang, Z. Resilient model of multi-UUVs cooperative localization for detection of sensor fault and outliers. *Ocean Eng.* **2022**, *266*, 113216. [CrossRef]
6. Zhou, Z.; Liang, X.; Shi, Z.; Wang, G.; Lang, J.; Liu, L. An improved comprehensive calibration method for ship strapdown inertial navigation system. *Ocean Eng.* **2023**, *269*, 113567. [CrossRef]
7. Xu, W.; Yang, J.; Wei, H.; Lu, H.; Tian, X.; Li, X. A localization algorithm based on pose graph using Forward-looking sonar for deep-sea mining vehicle. *Ocean Eng.* **2023**, *284*, 114968. [CrossRef]
8. Li, T.; Zhao, J.; Ma, J. A precise underwater positioning method by considering the location difference of transmitting and receiving sound waves. *Ocean Eng.* **2022**, *247*, 110480. [CrossRef]
9. Yang, L.; Zhao, S.; Wang, X.; Shen, P.; Zhang, T. Deep-Sea Underwater Cooperative Operation of Manned/Unmanned Submersible and Surface Vehicles for Different Application Scenarios. *J. Mar. Sci. Eng.* **2022**, *10*, 909. [CrossRef]
10. Cheng, C.; Wang, C.; Gao, L.; Zhang, F. Vessel and Underwater Vehicles Cooperative Localization using Topology Factor Graphs. In Proceedings of the OCEANS 2018 MTS/IEEE Charleston, Charleston, SC, USA, 22–25 October 2018; pp. 1–4. [CrossRef]
11. Wang, Q.; Fan, S.; Zhang, Y.; Gao, W.; Wei, J.; Wang, Y. A Novel Adaptive Sliding Observation-Based Cooperative Positioning Algorithm Under Factor Graph Framework for Multiple UUVs. *IEEE Trans. Ind. Inform.* **2022**, *19*, 8743–8753. [CrossRef]
12. Yan, Z.; Luan, Z.; Liu, J.; Xing, W. A Cooperative Localization Method for Multiple Unmanned Underwater Vehicles Based on Improved Factor Graph. In Proceedings of the 2023 IEEE International Conference on Mechatronics and Automation (ICMA), Heilongjiang, China, 6–9 August 2023; pp. 894–899.
13. Liang, Q.; Luo, M.; Wang, Y.; Hao, X. Multi-attacks effectiveness evaluation of UUV based on wake guidance. *Ocean Eng.* **2022**, *266*, 112654. [CrossRef]

14. Wu, Y.; Ta, X.; Xiao, R.; Wei, Y.; An, D.; Li, D. Survey of underwater robot positioning navigation. *Appl. Ocean. Res.* **2019**, *90*, 1845–1859. [CrossRef]
15. Wang, D.; Tang, E.; Li, L.; Peng, H.; Han, Y.; Chen, C.; Chang, M.; Guo, K.; He, L. Temperature and pressure propagation characteristics in multi-media interfaces of PVDF pressure sensor near underwater explosion source. *Ocean Eng.* **2023**, *287*, 115810. [CrossRef]
16. Yan, Z.; Zhou, T.; Guo, Q.; Xu, C.; Wang, T.; Peng, D.; Yu, X. Terrain matching positioning method for underwater vehicles based on curvature discrimination. *Ocean Eng.* **2022**, *260*, 111965. [CrossRef]
17. Zhang, L.; An, R. Least square estimation method for the navigation error of the UUVs. In Proceedings of the 2017 IEEE 9th International Conference on Communication Software and Networks (ICCSN), Guangzhou, China, 6–8 May 2017; pp. 775–778.
18. Wei, Y.; Yu, G.; Qu, F.; Sun, R. AUV-Aided Energy-Efficient Data Collection in Underwater Acoustic Sensor Networks. *IEEE Internet Things J.* **2020**, *7*, 10010–10022. [CrossRef]
19. Jia, Z.; Zheng, W.; Yuan, F. A Two-Dimensional Chirp-MFCSK Modulation Method for Underwater LoRa System. *IEEE Internet Things J.* **2022**, *9*, 24388–24397. [CrossRef]
20. Du, Z.; Wang, W.; Chai, H.; Xiang, M.; Zhang, F.; Huang, Z. Configuration analysis method and geometric interpretation of UUVs cooperative localization based on error ellipse. *Ocean Eng.* **2021**, *244*, 110299. [CrossRef]
21. TN, R.; Nherakkol, A.; Navelkar, G. Navigation of autonomous underwater vehicle using extended kalman filter. In *Trends in Intelligent Robotics: Proceedings of the 13th FIRA Robot World Congress, FIRA 2010, Bangalore, India, 15–17 September 2010*; Proceedings 13; Springer: Berlin Heidelberg, Germany, 2010; pp. 1–9. [CrossRef]
22. Zhang, F.; Wu, X.; Ma, P. Consistent Extended Kalman Filter-Based Cooperative Localization of Multiple Autonomous Underwater Vehicles. *Sensors* **2022**, *22*, 4563. [CrossRef]
23. Bai, M.; Huang, Y.; Chen, B.; Yang, L.; Zhang, Y. A Novel Mixture Distributions-Based Robust Kalman Filter for Cooperative Localization. *IEEE Sensors J.* **2020**, *20*, 14994–15006. [CrossRef]
24. Ullah, I.; Shen, Y.; Su, X.; Esposito, C.; Choi, C. A Localization Based on Unscented Kalman Filter and Particle Filter Localization Algorithms. *IEEE Access* **2019**, *8*, 2233–2246. [CrossRef]
25. Wang, Z.; Xiang, X.; Guan, X.; Pan, H.; Yang, S.; Chen, H. Deep learning-based robust positioning scheme for imaging sonar guided dynamic docking of autonomous underwater vehicle. *Ocean Eng.* **2024**, *293*, 116704. [CrossRef]
26. Peng, X.; Zhang, Y.; Xu, Z.; Zhang, Z.; Chen, L.; Li, C. PL-Net: Towards Deep Learning-Based Localization for Underwater Terrain. In *Neural Computing and Applications*; Springer: Berlin/Heidelberg, Germany, 2023; pp. 1–16. [CrossRef]
27. Zhu, J.; Kia, S.S. Learning-Based Measurement Scheduling for Loosely-Coupled Cooperative Localization. *IEEE Robot. Autom. Lett.* **2022**, *7*, 6313–6319. [CrossRef]
28. Liao, R.; Su, W.; Wu, X.; Cheng, E. Reinforcement Learning Based Mobile Underwater Localization for Silent UUV in Un-derwater Acoustic Sensor Networks. *Wirel. Commun. Mob. Comput.* **2022**, *2022*, 1–19. [CrossRef]
29. Brambilla, M.; Gaglione, D.; Soldi, G.; Mendrzik, R.; Ferri, G.; LePage, K.D.; Nicoli, M.; Willett, P.; Braca, P.; Win, M.Z. Co-operative Localization and Multitarget Tracking in Agent Networks with the Sum-Product Algorithm. *IEEE Open J. Signal Process.* **2022**, *3*, 169–195. [CrossRef]
30. Meyer, F.; Kropfreiter, T.; Williams, J.L.; Lau, R.; Hlawatsch, F.; Braca, P.; Win, M.Z. Message Passing Algorithms for Scalable Multitarget Tracking. *Proc. IEEE* **2018**, *106*, 221–259. [CrossRef]
31. Fan, S.; Zhang, Y.; Hao, Q.; Jiang, P.; Yu, C.; Yu, F. Cooperative Positioning for Multi-AUVs Based on Factor Graph and Maximum Correntropy. *IEEE Access* **2019**, *7*, 153327–153337. [CrossRef]
32. Zhang, L.; Wu, S.; Tang, C. Cooperative positioning of underwater unmanned vehicle clusters based on factor graphs. *Ocean Eng.* **2023**, *287*, 115854. [CrossRef]
33. Cheng, Y.; Wang, X.; Morelande, M.; Moran, B. Information geometry of target tracking sensor networks. *Inf. Fusion.* **2012**, *14*, 311–326. [CrossRef]
34. Tang, C.; Wang, Y.; Zhang, L.; Zhang, Y.; Song, H. Multisource Fusion UAV Cluster Cooperative Positioning Using Infor-mation Geometry. *Remote. Sens.* **2022**, *14*, 5491. [CrossRef]
35. Braca, P.; Goldhahn, R.; Ferri, G.; LePage, K.D. Distributed Information Fusion in Multistatic Sensor Networks for Underwater Surveillance. *IEEE Sensors J.* **2015**, *16*, 4003–4014. [CrossRef]
36. Ferri, G.; Munafò, A.; Tesei, A.; Braca, P.; Meyer, F.; Pelekanakis, K.; Petroccia, R.; Alves, J.; Strode, C.; LePage, K. Cooperative robotic networks for underwater surveillance: An overview. *IET Radar Sonar Navig.* **2017**, *11*, 1740–1761. [CrossRef]
37. Dell'Erba, R. Determination of Spatial Configuration of an Underwater Swarm with Minimum Data. *Int. J. Adv. Robot. Syst.* **2015**, *12*, 61035. [CrossRef]
38. dell'Erba, R. Distance estimations in unknown sea underwater conditions by power LED for robotics swarms. *Contin. Mech. Thermodyn.* **2021**, *33*, 97–106.
39. dell'Erba, R. The distances measurement problem for an underwater robotic swarm: A semi-experimental trial, using power LEDs, in unknown sea water conditions. *Contin. Mech. Thermodyn.* **2023**, *35*, 895–903.

40. Su, X.; Ullah, I.; Liu, X.; Choi, D. A Review of Underwater Localization Techniques, Algorithms, and Challenges. *J. Sensors* **2020**, *2020*, 1–24. [CrossRef]
41. Amari, S.I. *Information Geometry and Its Applications*; Springer: Berlin/Heidelberg, Germany, 2016.
42. Cover, T.M. *Elements of Information Theory*; John Wiley & Sons: Hoboken, NJ, USA, 1999.

Disclaimer/Publisher's Note: The statements, opinions and data contained in all publications are solely those of the individual author(s) and contributor(s) and not of MDPI and/or the editor(s). MDPI and/or the editor(s) disclaim responsibility for any injury to people or property resulting from any ideas, methods, instructions or products referred to in the content.